Development of Erythroid Progenitors under Erythropoietin Stimulation in Xenopus laevis Larval Liver

Authors: Okui, Takehito, Hosozawa, Sakiko, Kohama, Satoka, Fujiyama, Shingo, Maekawa, Shun, et al.

Source: Zoological Science, 33(6) : 575-582

Published By: Zoological Society of Japan

URL: https://doi.org/10.2108/zs160040

ZOOLOGICAL SCIENCE **33**: 575–582 (2016)

Development of Erythroid Progenitors Under Erythropoietin Stimulation in *Xenopus laevis* Larval Liver

Takehito Okui[1], Sakiko Hosozawa[1], Satoka Kohama[1], Shingo Fujiyama[1], Shun Maekawa[2], Hiroshi Muto[1], and Takashi Kato[1,2]*

[1]*Department of Integrative Bioscience and Biomedical Engineering, Graduate School of Advanced Science and Engineering, Center for Advanced Life and Medical Science, Waseda University, TWIns Building, 2-2 Wakamatsu-cho, Shinjuku-ku, Tokyo 162-8480, Japan*
[2]*Department of Biology, Faculty of Education and Integrated Arts and Sciences, Waseda University, TWIns Building, 2-2 Wakamatsu-cho, Shinjuku-ku, Tokyo 162-8480, Japan*

Erythroid progenitors that respond to erythropoietin (Epo) are present in the liver of adult *Xenopus laevis*. However, cells responding to Epo in the larval liver and through the metamorphosis period under hepatic remodeling have not been characterized. In this study, tadpoles were staged using the tables of Nieuwkoop and Faber (NF). Liver cells from pre- (NF56) or post- (NF66) metamorphic stage were cultured in the presence of Epo. *β2-globin* mRNA expression peaked at day 7 after the start of culture. Larval *β2-globin* was highly expressed in NF56-derived cells, while adult *β2-globin* was detected in those of NF66. In both NF56- and NF66-derived cells, mRNA expression of *epor* and *gata2* peaked at day 5 and days 3–4, respectively. In contrast, *gata1* expression peaked at day 6 in NF56 cells and at day 5 in NF66 cells. Half maximal proliferation of erythrocytic blast cells derived from the liver at NF66 was observed at day 3, which was earlier than that of NF56. These results indicate that erythroid progenitors that respond to *Xenopus laevis* Epo are maintained in pre- and post-metamorphic liver, although the tissue architecture changes dramatically during metamorphosis. Additionally, the *globin* switching occurred, and/or the erythroid progenitors for larval erythrocytes were replaced by those for adult erythrocytes in the metamorphic liver.

Key words: African clawed frog, tadpole, metamorphosis, liver, erythropoiesis, hematopoiesis, erythropoietin

INTRODUCTION

Erythropoietin (Epo) is a glycoprotein that is the major physiological regulator of erythropoiesis. Epo supports the survival of late erythroid progenitors and enhances their proliferation and differentiation by binding to Epo receptor (Epor) (Krantz, 1991; Jelkmann, 2010; D'Andrea and Zon, 1990). Epo stimulates burst-forming unit-erythroid cells (BFU-e) expressing Epor on the surface, and successively colony-forming unit-erythroid cells (CFU-e), at sites of erythropoiesis (Broudy et al., 1991; Gregory and Eaves, 1978; Sawada et al., 1987). Further, mature erythrocytes are produced through proerythroblasts, erythroblasts, and reticulocytes. The Epo dependency of erythroid progenitors varies with developmental stages (Boussios et al., 1989; Masuda et al., 1992; Emerson et al., 1989). Erythrocytes convert from primitive to definitive type in the fetal liver, a major site for the development of definitive erythrocytes (Koury et al., 2002; Isern et al., 2008).

During mammalian development, the hematopoietic system, including the embryonic yolk sac, liver, thymus, spleen, and bone marrow, is established in a continuous manner. As the hematopoietic organ changes during ontogeny, the nature of the hematopoietic microenvironment must also change (Orkin and Zon, 2008). The mechanism(s) involved in the transition of hematopoietic organs, however, are not well understood. The embryonic liver acts as a hematopoietic organ, unlike the adult liver, which performs various metabolic functions, such as serum protein synthesis, lipogenesis, detoxification, and urea synthesis (Oliver et al., 1983; Perry et al., 1983; Shelly et al., 1989; Orkin et al., 1996). As it acquires these metabolic functions, the embryonic liver loses its hematopoietic activity during late fetal development (Miyajima et al., 2000). Finally, hematopoietic cells move into the bone marrow or spleen around the perinatal stage to constitute the adult-type hematopoietic system.

In the African clawed frog, *Xenopus laevis* (*X. laevis*), hematopoiesis occurs first in the analog of yolk sac called the ventral blood island (VBI), and subsequently in the equivalent of the aorta-gonad-mesonephros (AGM) called the dorsal lateral plate (DLP) (Kau and Turpen, 1983; Flajnik et al., 1984; Maeno et al., 1985; Ciau-Uitz et al., 2000). Next, hematopoietic stem cells, which are derived from a part of VBI and DLP, migrate to the liver and maintain their hematopoietic activity until post-metamorphosis (Chen and Turpen, 1995; Turpen et al., 1997). During metamorphosis,

* Corresponding author. Tel. : +81-3-5369-7309;
Fax : +81-3-5369-7302;
E-mail: tkato@waseda.jp
doi:10.2108/zs160040

hemoglobin isoform switching changes the oxygen affinity in the liver (Mukhi et al., 2010); this process is physiologically important for the adaptation from an aquatic to a terrestrial habitat (Riggs, 1951). After metamorphosis, *X. laevis* grows into adulthood; however, unlike in mammals, in adult *X. laevis*, hematopoiesis does not occur in the bone marrow. Hepatic properties change during metamorphosis. For example, *fetuin B* and *alcohol dehydrogenase* are expressed in the pre-metamorphic stage, but their expression decreases in the post-metamorphic stage. Conversely, the expression of *albumin*, *cytochrome p450*, and *carbomyl phosphate synthetase* increase in the post-metamorphic stage (Mukhi et al., 2010). We previously identified cDNA sequences of *X. laevis* Epo (Nogawa-Kosaka et al., 2010) and Epor (Aizawa et al., 2005), and it has been shown that Epor-expressing cells localized to the inner wall of the sinusoid in the adult liver and Epo was mainly expressed in hepatocytes (Nogawa-Kosaka et al., 2011; Okui et al., 2013). Epo does not have an *N*-linked sugar chain, but exerts biological activity in vivo (Nogawa-Kosaka et al., 2010; Nagasawa et al., 2015), suggesting a paracrine action through the hepatic Epo-Epor pathway, similar to that in the fetal liver in mammals. Thus, hepatic erythropoiesis induced by the Epo-Epor pathway and the proliferation and differentiation of erythrocytes in adult *X. laevis* became clear. Likewise, thrombocyte progenitors reside in the liver and the spleen in *X. laevis* (Tanizaki et al., 2015). Therefore, the liver is one of the predominant multilineage hematopoietic organs. However, larval hematopoiesis remains to be elucidated, especially that at stages around the metamorphic climax approaching the adult stage.

In the present study, we examined erythroid progenitors that respond to Epo in the liver around metamorphic period at NF56 (pre-metamorphosis) and NF66 (post-metamorphosis). Developmental stages were classified based on the report of Nieuwkoop and Faber (1956). Epo stimulated the hepatic erythroid development toward hemoglobinized cells at NF56 and NF66. We further analyzed the differences in proliferation, morphology, and the expression of larval erythroid progenitors between NF56 and NF66 to understand the dynamics of *Xenopus* erythropoiesis from the metamorphic to the adult stage.

MATERIALS AND METHODS

Animals

Sexually mature adult *X. laevis* were purchased from an Aquatic Animal Supply (Misato, Japan). Tadpoles were obtained by the induction of breeding. For breeding, chorionic gonadotropin (hCG-Mochida, Mochida Pharmaceutical, Tokyo, Japan) was injected subcutaneously into adult *X. laevis*. Tadpoles were raised in a conventional culture room under light- (12-h/12-h light/dark cycle) and temperature- (22°C) controlled conditions. Green juice, including kale and green barley, was fed to the tadpoles at the pre-metamorphic stages, and fish food pellets were added after metamorphosis. All animal experiments in this study were conducted in accordance with the Regulations for Animal Experimentation of Waseda University, Tokyo, Japan. Larvae were staged based on the definition of Nieuwkoop and Faber (Nieuwkoop and Faber, 1967).

Histology

Tadpoles were anesthetized with 1 mg/L of ethyl 3-aminobenzoate methanesulfonate (MS-222; Sigma-Aldrich, St Louis, MO, USA) in ice-cold water. The livers were immediately collected from anesthetized tadpoles. Tissue samples were fixed for 24 hours at 4°C in Bouin's solution (Sigma-Aldrich, St Louis, MO, USA), dehydrated through a graded series of ethanol, embedded in Paraplast (Kendall-Tyco Healthcare, Mansfield, MA, USA) and cut into 4-μm thick sections. The sections were stained with hematoxylin-eosin solution (Wako Pure Chemical Industries, Osaka, Japan) and mounted with Bioleit (Okenshoji, Tokyo, Japan).

Cytology

Dulbecco's modified phosphate-buffered saline without Mg^{2+} and Ca^{2+} ions (dDPBS (–)) was used to avoid blood coagulation. Cytocentrifuged preparations were made with 2×10^5 cells diluted in 0.8 × dDPBS (–), containing 50% fetal calf serum (FCS) (AusGeneX, Brisbane, Australia). The cell suspension was centrifuged at 1,100 × *g* for four minutes onto glass slides. After air drying, preparations were fixed for 5 minutes in methanol, incubated in 0.1% *o*-dianisidine (Wako Pure Chemical Industries, Osaka, Japan) in methanol, incubated 30% hydrogen peroxide for 1.5 minutes, washed in running water, and counterstained with Giemsa solution (Okui et al., 2013).

Cell culture

The isolation of hematopoietic progenitor cells from the liver was performed as previously described (Nogawa-Kosaka et al., 2011). Briefly, livers were dissected and placed in 0.8 × dDPBS (–) or 0.8 × alpha minimum essential medium (α-MEM) (Invitrogen, Carlsbad, CA, USA). Organs were washed, minced, and drawn in and out of a syringe through a 27 gauge needle, and treated with a hemolysis solution (150 mM NH_4Cl, 14 mM $NaHCO_3$, 0.12 mM EDTA-2Na) to remove most erythrocytes. To prepare a single-cell suspension, the cell suspension was further filtered through a 40-μm nylon cell strainer (BD Biosciences, San Jose, CA, USA). Cells (1.5×10^4) were cultured in 0.8 × α-MEM including 10% heat-inactivated FCS, streptomycin (Invitrogen, Carlsbad, CA, USA), penicillin (Invitrogen, Carlsbad, CA, USA), and 1% adult *X. laevis* serum in 96-well plates. Epo produced by *Escherichia coli* was added to culture medium. The assay for cell proliferation was conducted in the presence of 100 ng/ml Epo in accordance with the protocol of a

Table 1. Sequences of primers for RT-PCR.

gene	gene name (Xenbase)	sequence
larval *β2-globin*	*hemoglobin subunit gamma 2*	Fw 5'-ACCCCTGGACCCAGAGATAC-3'
		Re 5'-CATTGCCAACAGCTGAAAGA-3'
adult *β2-globin*	*hemoglobin subunit gamma 2*	Fw 5'-CCATCAAGCACATGGATGAC-3'
		Re 5'-GAGCCAGGGCAATAGACAAG-3'
epo	*erythropoietin*	Fw 5'-TGTTCGTTAGTGTGAAGCTCGT-3'
		Re 5'-GAGACCGTTCCAAACCTCTG-3'
epor	*erythropoietin receptor*	Fw 5'-GCTGCACTTCCACAATCTTTC-3'
		Re 5'-CACTCTGTTGTTTGCCTTTACTG-3'
gapdh	*glyceraldehyde-3-phosphate dehydrogenase*	Fw 5'-ATGGTGAAGGTTGGAATTAACGG-3'
		Re 5'-GACAGGTGACAAGTGCTTATTCC-3'
gata1	*GATA binding protein 1*	Fw 5'-CCAAAGAAACGCCTGATTGT-3'
		Re 5'-TCTCCACTTGCATTCCGTC-3'
gata2	*GATA binding protein 2*	Fw 5'-ACAGCAGCGGCCTCTTTCATC-3'
		Re 5'-CCGGTCCCATCTCTTCTCCAC-3'
rpl13a	*ribosomal protein L13a*	Fw 5'-GGCAACTTCTACCGCAACAA-3'
		Re 5'-GTCATAGGGAGGTGGGATTCC-3'

previous report (Nogawa-Kosaka et al., 2011). Cells on each day were stained with Trypan Blue solution and counted with a hemocytometer.

Reverse transcription polymerase chain reaction (RT-PCR)

Total RNA was extracted from cells on each culturing day and whole liver using TriPure Isolation Reagent (Roche Applied Science, Indianapolis, IN, USA) according to manufacturer's instructions. Total RNA was reverse-transcribed into cDNA using ReverTra Ace (Toyobo, Osaka, Japan). Fragments of *ribosomal protein l13a* (*rpl13a*) and *glyceraldehyde-3-phosphate dehydrogenase* (*gapdh*) were amplified as an internal standard by reference to a previous study (Nogawa-Kosaka et al., 2010). The primer sequences were listed in Table 1. For genes and proteins of *X. laevis*, we followed the notation method declared in Xenbase (http://www.xenbase.org/gene/static/geneNomenclature.jsp).

Statistical analysis

All experiments were performed in triplicate. Error bars in figures show standard errors. Student's *t*-test and Dunnett's test were used when appropriate. Results which p-values were under 0.05 were considered to be significant.

RESULTS

Liver structure at the metamorphic stage

At NF56, the length of the body reached approximately 30 mm under our breeding conditions. Forelimb and hind limb were formed clearly, and elimination of the caudal portion started at NF60 (middle metamorphic stage). At the climax of metamorphosis (NF66), caudal elimination was complete, and the body morphology transformed to that of adult frogs (Fig. 1A). In the metamorphic stages, from NF56 to NF66, changes occurred in both the external morphology and the internal structure. The lung could be observed at NF56, and tissue arrangement of the intestine, which was in a spiral configuration at NF56, changed to a more complicated structure at NF66. Sternum formation began at NF60. From NF56 to NF60, larval liver increased in size and turned red (Fig. 1B).

The structure of the liver changed greatly during metamorphosis. The number of lobes varied from three at NF56 to two at NF66. HE-stained liver sections at NF49, 56, 60, and 66 clearly demonstrated the morphological changes in hepatocytes and the increase in sinusoid diameter (Fig. 1C). At NF49, the structure of the hepatic cell cord was unclear, and the diameter of the sinusoid was wider than that at NF56, 60, and 66. It is known that the pigment cells, melanomacrophages, appear in adult liver (Wiechmann et al., 2003). Melanomacrophages were not observed in the liver at NF49 and NF56, and they began to appear at NF60 (Fig. 1C). The staining property also changed during the development, and the area of sinusoid decreased from NF56 (Fig. 1D). The size of hepatocytes increased significantly at NF66 (Fig. 1E). We then examined

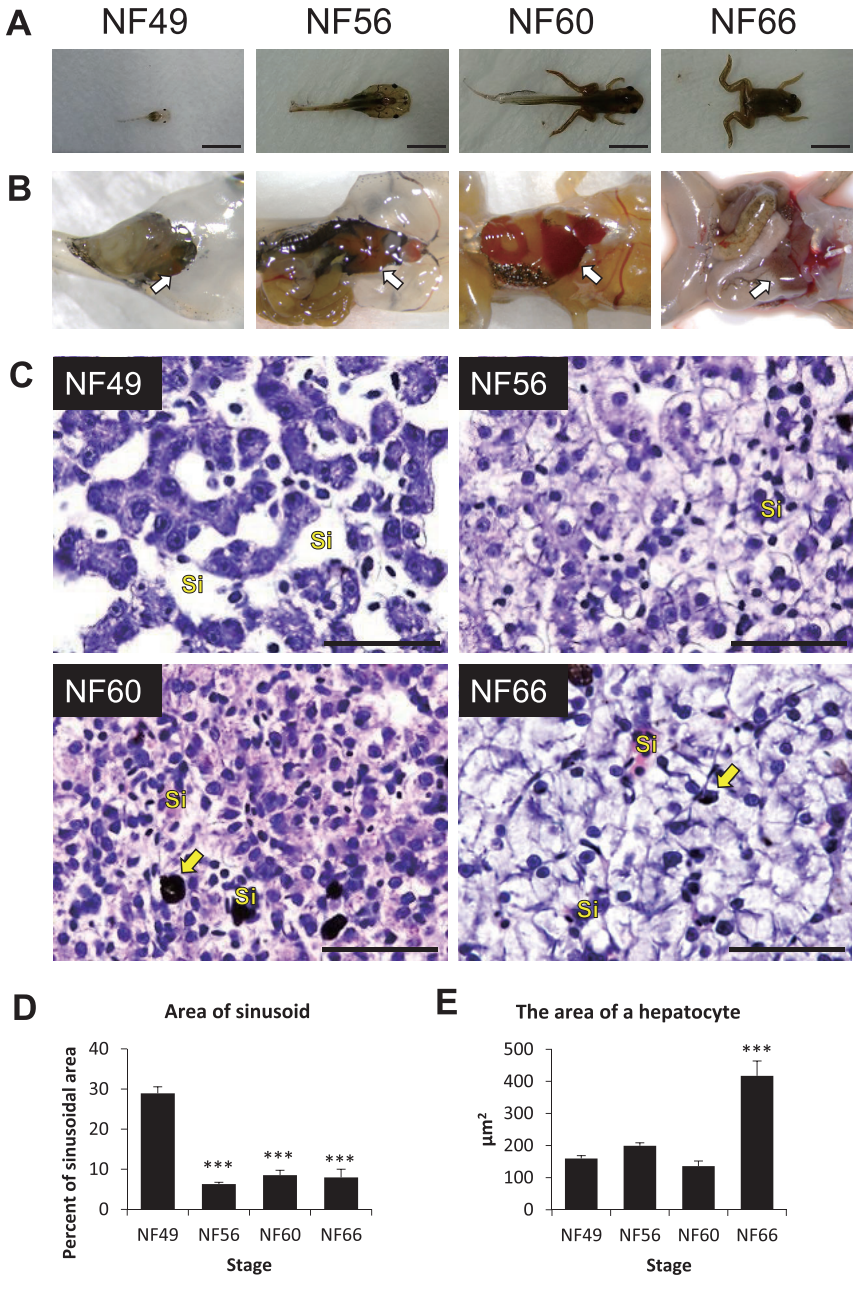

Fig. 1. **(A)** Comparison of liver structure at different metamorphic stages; NF49, 56, 60, and 66 are shown. Scale bars represent 10 mm. **(B)** Internal organs at stages NF49, 56, 60, and 66 from the ventral direction are shown. The directions of bodies are same as that seen in **(A)**. Arrows indicate the liver. **(C)** Paraffin-embedded liver sections (4-μm thickness) at NF49, 56, 60, and 66, stained with HE solution. Yellow arrows show melanomacrophages. Scale bars represent 50 μm. Si; sinusoid. **(D)** Ratios of sinusoidal area in one visual field in NF49, 56, 60, 66 livers. Values represent means (n = 3), and error bars represent standard errors. **(E)** The area of a hepatocyte of NF49, 56, 60, 66 are shown. Values represent means (n = 3), and error bars represent standard errors. ***; $P < 0.001$, Dunnett's test (vs. NF49).

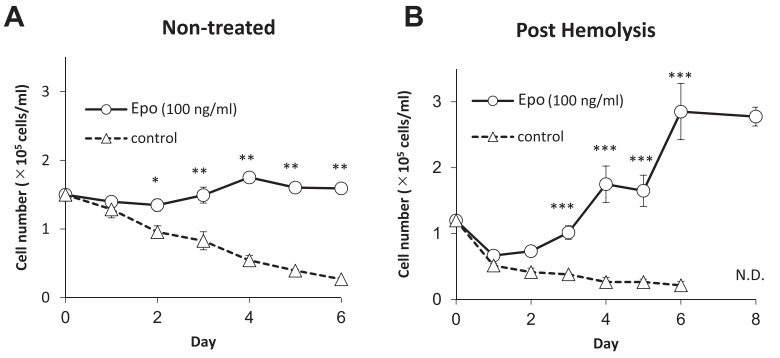

Fig. 2. Difference in cell proliferation after hemolysis processing. **(A)** Whole liver cells of NF56 were cultured in the presence of Epo (100 ng/ml). Values represent means (n = 3), and error bars represent standard errors. Circles show 100 ng/ml Epo. The dashed line indicates the control group. *; $P < 0.05$, **; $P < 0.01$, Student's t-test (vs. control). **(B)** Liquid culture of liver cells at NF56 with Epo. Cells were treated with hemolysis solution. The sequential cell counts of viable cells are shown. Values represent means (n = 3), and error bars represent standard errors. Solid lines indicate the number of cells, which are cultured with Epo (100 ng/ml), and the dashed line indicates the control. *; $P < 0.05$, **; $P < 0.01$, ***; $P < 0.001$, Student's t-test (vs. control). N.D.; not detected.

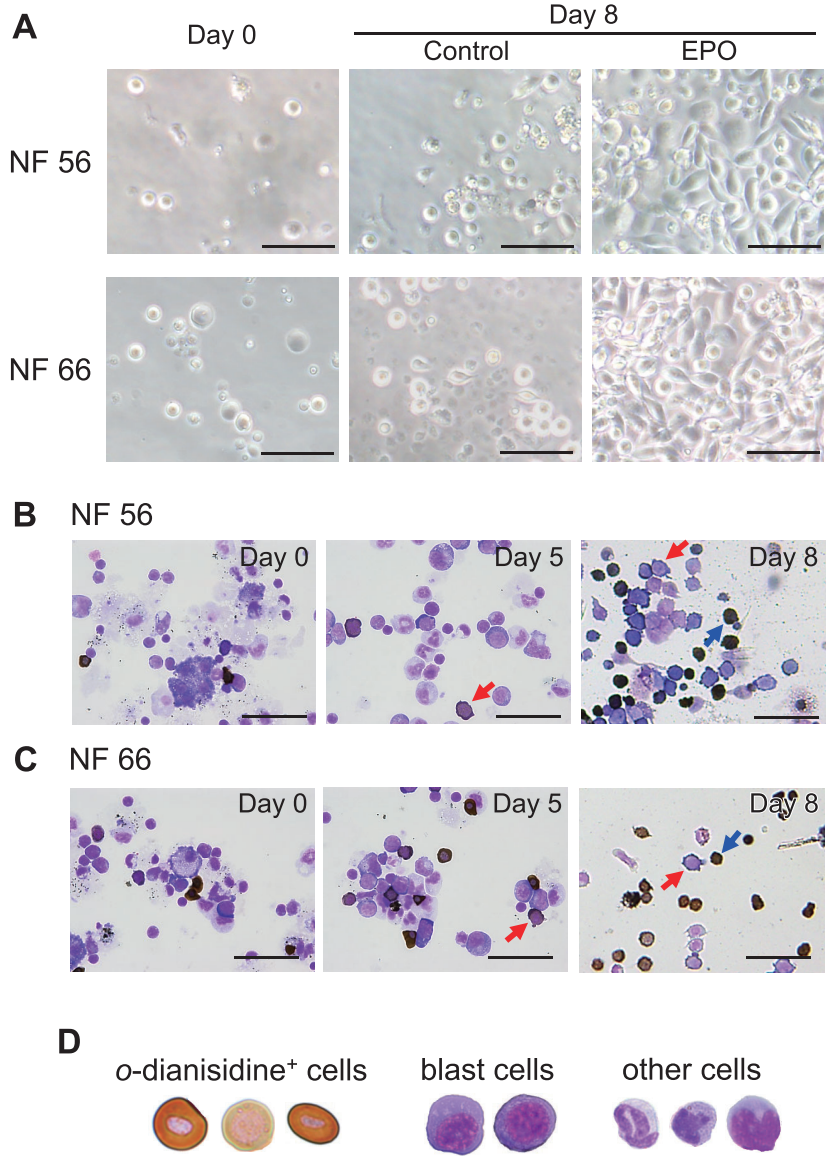

Fig. 3. Morphology of the liver cells cultured with Epo. **(A)** Micrographs of liquid cultured cells at day 0 (left column) and day 8 control and Epo (middle and left column, respectively) are shown. Scale bars represent 50 μm. **(B, C)** Liquid-cultured cells of NF56 **(B)** and NF66 **(C)** livers were treated with *o*-dianisidine and Giemsa solution on day 0, day 5, and day 8. Red arrows indicate blast cells, and blue arrows indicate the *o*-dianisidine⁺ cells. Scale bars represent 50 μm. **(D)** Morphological typing of cultured cells. Cells were treated with o-dianisidine solution, and stained with Giemsa solution for counter staining. The *o*-dianisidine⁺ cells, blast cells, and other cells were defined.

erythroid progenitors in the liver during the metamorphic period and evaluated their response to Epo.

Reactivity of pre- and post-metamorphic liver cells to Epo

When whole liver cells of NF56 larvae were cultured in the presence of Epo, the survival rates of the cells increased from that of the control, but the cell counts did not increase (Fig. 2A). Since it was possible that mature erythrocytes express Epor to avoid apoptosis due to Epo-Epor signaling (Aizawa et al., 2005; Tamura et al., 2015), we removed mature erythrocytes by hemolysis prior to liquid culture. This also suppressed the absorption of unbound Epo to Epor in the culture. After removal of mature erythrocytes by hemolysis, the number of proliferating cells increased (Fig. 2B).

Previous studies have shown that erythropoiesis takes place in the liver of tadpoles; therefore, we examined whether erythroid progenitors that responded to Epo resided in the larval liver. When larval hepatic cells at NF56 or NF66 were cultured in the presence of Epo, the cells proliferated, and several types of erythrocytic cells emerged in the respective cultures at day 8 (Fig. 3A). To characterize the types of erythrocytic cells induced by stimulation by Epo, we stained the cultured cells on each day with *o*-dianisidine to classify them based on hemoglobinization. A number of blast cells and pale brown cells that appeared on day 5 were not validated as erythrocytic cells. Subsequently, mature erythrocytes emerged abundantly at day 8 from liver cells at both NF56 and NF66 (Fig. 3B and 3C). Next, viable blast cells and mature erythrocytes from liver cells at NF56 or NF66 were counted on each culture day. We classified cultured cells into three cell subpopulations based on the size of nuclei and the results of *o*-dianisidine and Giemsa staining: (1) mature erythrocytes robustly stained with *o*-dianisidine (brown cytoplasm), (2) blast cells with large nuclei (blue or very

pale brown cytoplasm stained with Giemsa and *o*-dianisidine), and (3) other cells with lobulated nuclei (negative to *o*-dianisidine-staining) (Fig. 3D).

The viable cells increased in the cultures of the liver cells of NF56 and NF66 (Fig. 4A, B). In the culture of the cells derived from the NF56 liver, half maximal of the number of viable cells was attained at 5 days and the maximal was attained at day 7 after the start of culture (Fig. 4A). At NF66, the cell number did not reach the maximum plateau until day 8 (Fig. 4B). The difference in the pattern of cell proliferation between NF56 and NF66 was that the NF56 cells increased in a sigmoid pattern, while NF66 cells expanded in a linear pattern. Dead cell counts for NF56 and NF66 were similar to those for the control (data not shown).

Blast cell numbers at both NF56 and NF66 started to increase at day 3, peaked at day 5 (NF56) and day 4 (NF66), and then decreased at day 7 (Fig. 4C, D). The number of *o*-dianisidine$^+$ cells decreased by day 5 for NF56, while a slight rise was observed at day 2 for NF66 (Fig. 4C, D). However, a rapid increase was observed at day 7 (NF56) and day 6 (NF66). Additionally, at day 8, the number of *o*-dianisidine$^+$ cells continued to increase for NF66, while it decreased for NF56. In the light of cell proportion in the culture of both NF56- and NF66-derived cells, blast cells increased at first, and *o*-dianisidine$^+$ cells increased thereafter, then blast cells decreased (Fig. 4E, F).

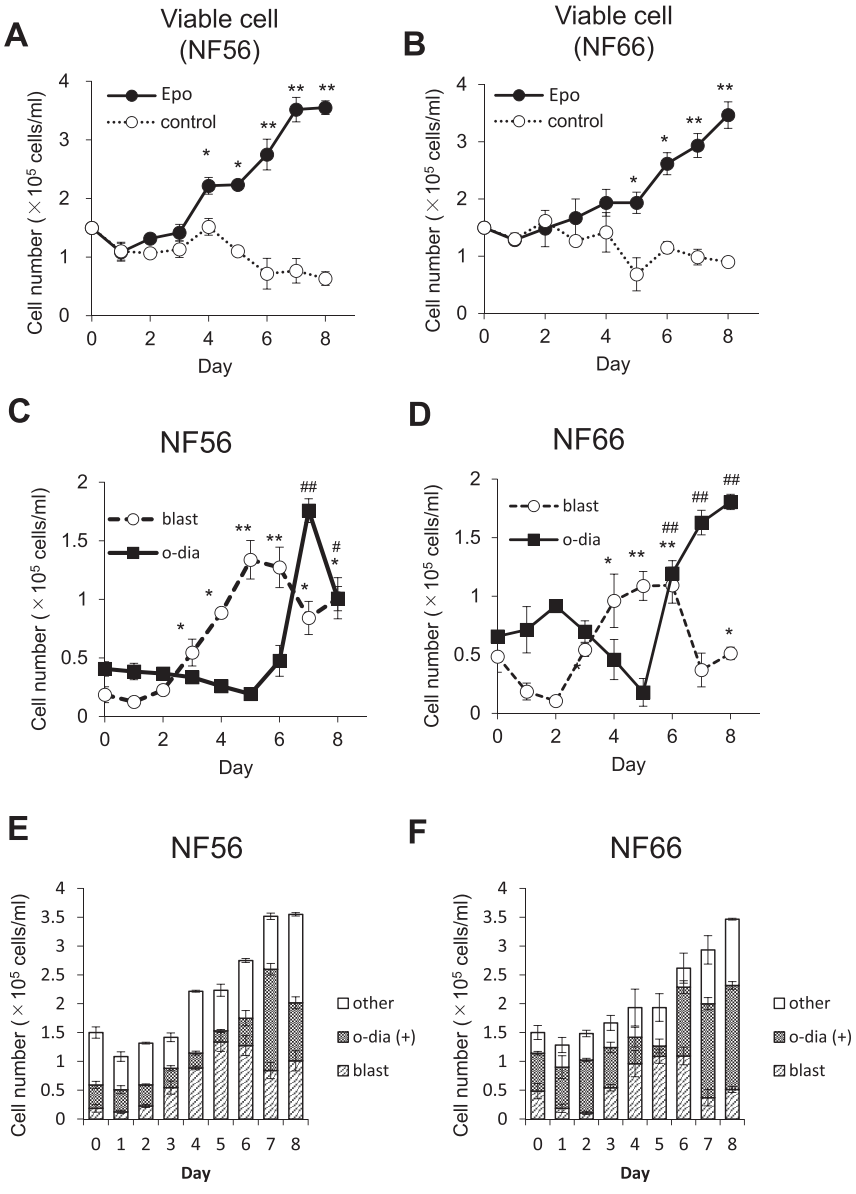

Fig. 4. Liquid culture of liver cells at NF56 and NF66 with Epo. **(A, B)** Sequential cell counts of viable cells from NF56 **(A)** and NF66 **(B)** are shown. Values represent means (n = 3, * $P < 0.05$, ** $P < 0.01$), and error bars represent standard errors. Solid lines indicate the number of cells which are cultured with Epo, and dashed lines are control. **(C, D)** The sequential cell counts of blast cells and *o*-dianisidine$^+$ cells from NF56 **(C)** and NF66 **(D)** liver cells are shown. Values represent means (n = 3, *, # $P < 0.05$, **, ## $P < 0.01$ vs. control, Student's t-test), and error bars represent standard errors. Dash lines indicate the number of blast cells, and solid lines indicate the number of *o*-dianisidine$^+$ cells. **(E, F)** The sequential change of cell components in the culture. Blast cells (shaded area), *o*-dianisidine$^+$ cells (dotted area), and other cells (blank area) were counted and represented in stacked bar graphs. Values represent means (n = 3), and error bars represent standard errors.

Gene expression in pre- and post-metamorphic tissues

In adult *X. laevis*, the liver is the predominant hematopoietic organ (Hadji-Azimi et al., 1987; Nogawa-Kosaka et al., 2011). The whole liver at NF56 and NF66 expressed *epo*, *epor*, *gata2*, and *gata1* (Fig. 5A). To characterize the cells responding to Epo, the expression of various genes at each day was analyzed by RT-PCR (Fig. 5B, C). We evaluated the mRNA expression of Epor and Gata, which participate in erythropoiesis in mammals and fish. We first examined the Gata-binding regions on the *X. laevis globin* gene (data not shown). In the NF56 and NF66 liver cells cultured in the presence of Epo, the expression of both larval and adult *globin* were up-regulated at days 6–8, consistent with the growth pattern of *o*-dianisidine$^+$ cells. Interestingly, the expression of larval or adult *globin* gene increased predominantly in NF56- and NF66-derived cells, respectively. The wavy change of *globin* expression was detected in the culture (Fig. 5B, C). Both larval and adult *globin* were expressed initially in the cultures NF56 and NF66 liver cells, and their expression levels gradually declined to the nadir at around day 4, and then the expression levels increased again at day 6. The expression of *epor* reached a peak in both liver cultures (NF56 and NF66) as erythrocytic blast cells expressing *epor* emerged. Similar to *globin* expression, the expression of *epor* was detected at day 0, decreased to the nadir at days 1–2, and then increased to reach a peak at

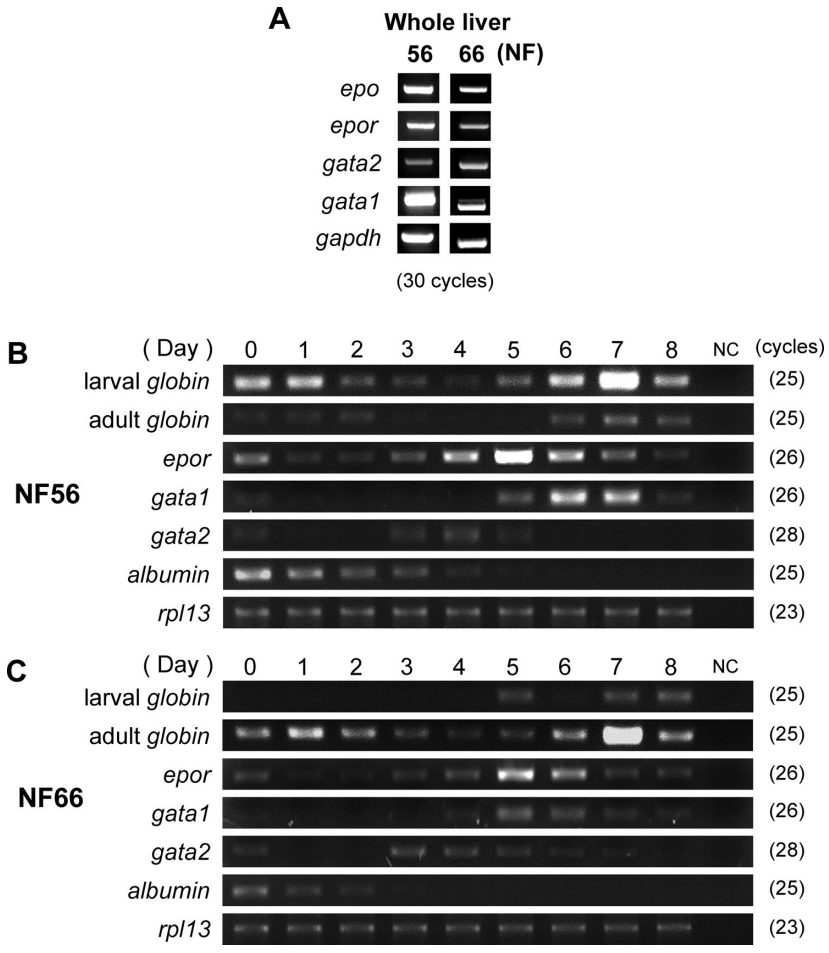

Fig. 5. Gene expressions of *epo*, *epor*, *gata2*, and *gata1* in whole liver of NF56 and NF66 were shown **(A)**. *Gapdh* was used as an internal control. Gene expressions of liquid cultured liver cells at NF56 **(B)** and NF66 **(C)**. Sequential gene expressions of liquid-cultured cells at NF56 and NF66 are shown for **(B)** and **(C)**, respectively. *Rpl13A* was used as an internal control.

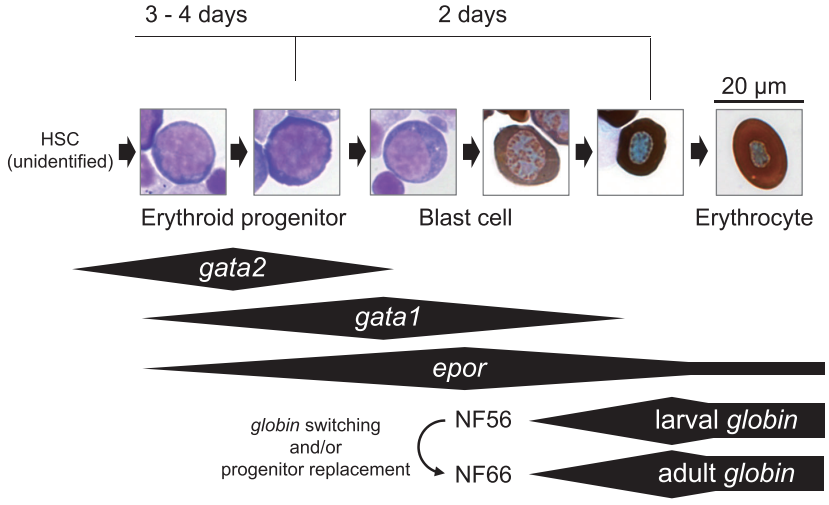

Fig. 6. Conceptual diagram of erythropoiesis with morphology and gene expression in *X. laevis*. *Gata2* expressed highly in days 3–4. After a day from the peak of *gata2* expression, *gata1*, and *epor* expressed highly, and differentiated into erythroblasts like mammals. Furthermore, erythroblasts accumulated larval or adult hemoglobin over about two days and differentiated into mature erythrocytes.

around day 3. The expression of *gata2* was detected at days 3–4 (NF56 and NF66). The expression of *gata1* peaked at day 6 in the NF56 liver cells, while that in NF66 liver cells peaked at day 5. The peak of *gata1* expression was reached about 2 days after that of *gata2*. *Albumin* expression was observed in the early culture days, and it showed a sequential decline, indicating that exogenous Epo could not maintain hepatocyte culture under this condition. The changes in gene expression over the course of erythroid development are shown in Fig. 6.

DISCUSSION

The liver of *X. laevis* has been thought to function as a hematopoietic organ in both larva and adult. However, it has been shown that the properties of the liver change throughout the metamorphic period (Mukhi et al., 2010), suggesting that the hematopoietic environment differs in larval and adult tissues. The key findings of the present study are: (1) erythroid progenitors remain in the liver, despite dramatic changes in the environment and tissue organization during the metamorphosis period and (2) larval hepatic erythroid progenitors at pre- and post-metamorphic stages respond differently to Epo. It is known that hematopoiesis is closely associated with the hematopoietic "niche" in the tissue microenvironment (Suda et al., 2005; Miyajima et al., 2000). During metamorphosis, the size and shape of hepatocytes, the diameter of sinusoid, staining properties, and the number of erythrocytes in the liver varied greatly (Fig. 1C–E). In this study, we found that erythroid progenitors exist in the larval liver. The structure and function of the liver undergoes significant changes during the pre- and post-metamorphosis stages (Fig. 1B) (Brown and Cai, 2007).

We also investigated whether the properties of hepatic erythroid progenitors changed in response to the transmutation of the niche. Previous studies have shown that erythropoiesis occurs through the Epo-Epor system in adult *X. laevis* (Nogawa-Kosaka et al., 2011); however, the mechanism in *X. laevis* larvae has remained unclear. We revealed in the present study that the erythroid progenitors in the larval liver proliferated and matured under recombinant Epo stimulation. The number of blast cells with large nucleus and blue-stained cytoplasm (Fig. 3) increased in the presence of Epo, which was consistent with the *epor* expression pattern, demonstrating that these blast cells were erythroblasts. The number of *o*-dianisidine$^+$ cells was higher than that of blast cells at respective peak days, indicating that blast

cells had the capacity to mature in the presence of Epo. The transcription factors GATA2 and GATA1 play key roles in erythroid development in mammals (Doré et al., 2011). Their expressions are strictly regulated in the erythroid lineage. We observed the expression period of *gata1* and *gata2* changed sequentially, suggesting that their expression was controlled at stages of erythroid development and differentiation in the analogous way of mammals. The crossover in the expression of larval and adult *globin* mRNAs between NF56 and NF66 under stimulation with Epo indicated the difference in the properties of erythroid progenitors undergoing differentiation. The timing of the initiation of blast cell proliferation was also different for NF56 and NF66. This suggested that the progenitor cells residing in NF56 liver may be more immature than those at NF66; therefore, the NF66 liver cells responded to Epo sooner than NF56 liver cells.

The gene expression profiles of larval liver and cultured hepatic cells were also analyzed in this study. The larval whole liver expressed *epo* at pre- (NF56) and post- (NF66) metamorphosis (Fig. 5A) similar to that in adult *X. laevis* (Nogawa-Kosaka et al., 2010). This finding is consistent with *epo* expression in the liver of NF57, 60, 62, and 64 reported previously (Tamura et al., 2015). This expression is probably derived from hepatocytes like adult *X. laevis* (Nogawa-Kosaka et al., 2010). In addition, *epor*, *gata2*, and *gata1* were also detected in the whole liver of NF56 and NF66 (Fig. 5A). In adult frogs, Epo has been suggested to bind to Epor through a paracrine system in the liver (Nogawa-Kosaka et al., 2010). The same erythropoietic system likely exists in larvae, as suggested by the expression of Epo mRNA in the larval liver. The expression of *globin* and *epor* was observed early in culture, after which their expression levels declined gradually (Fig. 5B, C). It is possible that the *globin* and *epor* mRNAs detected at the early stages were produced by the originally developed hepatic erythrocytes or progenitors, although we removed erythrocytes by hemolyzing before seeding cells. In the culture of NF56 liver cells, *gata2* expression peaked at day 4, and *gata1* expression reached a peak at day 6. This suggests that the erythroid progenitors expressing *gata2* differentiated into erythroblasts expressing *gata1* (Fig. 6). In the culture of NF66 liver cells, *gata2* expression peaked at day 3, and *gata1* expression reached a peak at day 5. The difference in the time of reaching maximal expression for *gata2* and *gata1* between NF56 and NF66 indicated that the hematopoietic cells residing in the liver of NF56 and NF66 were at different stages of development. The life span of larval developing erythrocytes compared to that of adult ones remains to be addressed, as larval type erythrocytes are replaced by adult type erythrocytes. The life span of erythrocytes was 20 to 40 days in mice (Burwell et al., 1953; Van Putten and Fineke, 1958), while it is approximately 220 days in adult *X. laevis* (Maekawa et al., 2012). In contrast, the life span of the erythrocytes derived at various developmental stages from larval livers is unknown.

In fish, the kidney is a major hematopoietic organ, as has been reported in zebrafish (Davidson and Zon, 2004). Furthermore, a variety of hematopoietic organs have been reported among animals. In addition, a transition of the hematopoietic organs in accordance to ontogenic stage has also been observed in many animals. *Xenopus laevis* may thus represent a useful animal model for elucidating the functions/characteristics of the hematopoietic niche, as hematopoiesis occurs consistently in its liver throughout its lifetime from tadpole to adult frog. In this regard, the culture system for larval liver cells used in this study is well-suited to analyses of the changes that occur during metamorphosis with respect to erythrocyte development.

In conclusion, erythroid progenitors that respond to Epo were maintained in pre- and post-metamorphic liver, although the tissue architecture changed dramatically during metamorphosis. The erythroid progenitors for larval erythrocytes were replaced by adult erythrocytes in the post-metamorphic liver.

ACKNOWLEDGMENTS

We thank Mr. Kazuo Ouchi for advice on breeding technique. We also thank Dr. Yusuke Yamamoto for constructive advice. This work was supported in part by Grants-in-Aid for Scientific Research (KAKENHI) from the Japan Society for the Promotion of Science (No. 20570063 and 26440171), Grants for Special Research Project from Waseda University (No. 2007B-061, 2011B-047, 2012B-045 and 2013B-056) and by “High-Tech Research Center” Project for Private Universities: matching fund subsidy from the Ministry of Education, Culture, Sports, Science and Technology (MEXT) (No. 07H016). A part of this study was performed as MEXT-Supported Program for the Strategic Research Foundation at Private Universities.

REFERENCES

Aizawa Y, Nogawa N, Kosaka N, Maeda Y, Watanabe T, Miyazaki H, Kato T (2005) Expression of erythropoietin receptor-like molecule in *Xenopus laevis* and erythrocytopenia upon administration of its recombinant soluble form. J Biochem 138: 167–175

Ashley H, Katti P, Frieden E (1968) Urea excretion in the bullfrog tadpole: effect of temperature, metamorphosis, and thyroid hormones. Dev Biol 17: 293–307

Boussios T, Bertles JF, Goldwasser E (1989) Erythropoietin: receptor characteristics during the ontogeny of hamster yolk sac erythroid cells. J Biol Chem 264: 16017–16021

Broudy VC, Lin N, Brice M, Nakamoto B, Papayannopoulou T (1991) Erythropoietin receptor characteristics on primary human erythroid cells. Blood 77: 2583–2590

Brown DD, Cai L (2007) Amphibian metamorphosis. Dev Biol 306: 20–33

Chen XD, Turpen JB (1995) Intraembryonic origin of hepatic hematopoiesis in *Xenopus laevis*. J Immunol 154: 2557–2567

Ciau-Uitz A, Walmsley M, Patient R (2000) Distinct origins of adult and embryonic blood in *Xenopus*. Cell 102: 787–796

D’Andrea AD, Zon LI (1990) Erythropoietin receptor. Subunit structure and activation. J Clin Invest 86: 681–687

Davidson AJ, Zon LI (2004) The ‘definitive’ (and ‘primitive’) guide to zebrafish hematopoiesis. Oncogene 23: 7233–7246

Doré LC, Crispino JD (2011) Transcription factor networks in erythroid cell and megakaryocyte development. Blood 118: 231–239

Emerson SG, Thomas S, Ferrara JL, Greenstein JL (1989) Developmental regulation of erythropoiesis by hematopoietic growth factors: Analysis on populations of BFU-E from bone marrow, peripheral blood, and fetal liver. Blood 74: 49–55

Flajnik MF, Horan PK, Cohen N (1984) A flow cytometric analysis of the embryonic origin of lymphocytes in diploid / triploid chimeric *Xenopus laevis*. Dev Biol 104: 247–254

Fraser ST, Isern J, Baron MH (2007) Maturation and enucleation of primitive erythroblasts is accompanied by changes in cell surface antigen expression patterns during mouse embryogenesis. Blood 109: 343–352

Frieden E, Herner AE, Fish L, Lewis EJC (1957) Changes in serum proteins in amphibian metamorphosis. Science 126: 559–560

Gregory CJ, Eaves AC (1978) Three stages of erythropoietic progenitor cell differentiation distinguished by a number of physical and biologic properties. Blood 51: 527–537

Hadji-Azimi I, Canicatti C (1987) Atlas of adult *Xenopus laevis* hematology. Dev Comp Immunol 11: 807–874

Isern J, Fraser ST, He Z, Baron MH (2008) The fetal liver is a niche for maturation of primitive erythroid cells. Proc Natl Acad Sci U S A 105: 6662–6667

Jelkmann W (2010) Biosimilar epoetins and other "follow-on" biologics: update on the European experiences. Am J Hematol 85: 771–780

Kau C, Turpen JB (1983) Dual contribution of embryonic ventral blood island and dorsal lateral plate mesoderm during ontogeny of hematopoietic cells in *Xenopus laevis*. J Immunol 131: 2262–2266

Koury MJ, Sawyer ST, Brandt SJ (2002) New insights into erythropoiesis. Curr Opin Hematol 9: 93–100

Krantz SB (1991) Erythropoietin. Blood 77: 419–434

Maeno M, Tochinai S, Katagiri C (1985) Differential participation of ventral and dorsolateral mesoderms in the hemopoiesis of *Xenopus*, as revealed in diploid-triploid or interspecific chimeras. Dev Biol 110: 503–508

Masuda S, Hisada Y, Sasaki R (1992) Developmental changes in erythropoietin receptor expression of fetal mouse liver. FEBS lett 298: 169–172

Miyajima A, Kinoshita T, Tanaka M, Kamiya A, Mukouyama Y, Hara T (2000) Role of Oncostatin M in hematopoiesis and liver development. Cytokine Growth Factor Rev 11: 177–183

Mukhi S, Cai L, Brown DD (2010) Gene switching at *Xenopus laevis* metamorphosis. Dev Biol 338: 117–126

Munro AF (1939) Nitrogen excretion and arginase activity during amphibian development. Biochem J 33: 1957–1965

Nagasawa K, Meguro M, Sato K, Tanizaki Y, Nogawa-Kosaka N, Kato T (2015) The influence of artificially introduced *N*-glycosylation sites on the in vitro activity of *Xenopus laevis* erythropoietin. PLoS One 10(4): e0124676

Nieuwkoop P, Faber J (1956) Normal table of *Xenopus laevis* (Daudin). Elsevier/North-Holland, New York

Nishikawa A, Hayashi H (1999) T3-hydrocortisone synergism on adult-type erythroblast proliferation and T3-mediated apoptosis of larval-type erythroblasts during erythropoietic conversion in *Xenopus laevis*. Histochem Cell Biol 111: 325–334

Nogawa-Kosaka N, Hirose T, Kosaka N, Aizawa Y, Nagasawa K, Uehara N, et al. (2010) Structural and biological properties of erythropoietin in *Xenopus laevis*. Exp Hematol 38: 363–372

Nogawa-Kosaka N, Sugai T, Nagasawa K, Tanizaki Y, Meguro M, Aizawa Y, et al. (2011) Identification of erythroid progenitors induced by erythropoietic activity in *Xenopus laevis*. J Exp Biol 214: 921–927

Okui T, Yamamoto Y, Maekawa S, Nagasawa K, Yonezuka Y, Aizawa Y, Kato T (2013) Quantification and localization of erythropoietin-receptor-expressing cells in the liver of *Xenopus laevis*. Cell Tissue Res 353: 153–164

Oliver IT, Martin RL, Fisher CJ, Yeoh GC (1983) Enzymic differentiation in cultured foetal hepatocytes of the rat. Induction of serine dehydratase activity by dexamethasone and dibutyryl cyclic AMP. Differentiation 24: 234–238

Orkin SH (1996) Development of the hematopoietic system. Curr Opin Genet Dev 6: 597–602

Orkin SH, Zon LI (2008) Hematopoiesis: An evolving paradigm for stem cell biology. Cell 132: 631–644

Riggs A (1951) The metamorphosis of hemoglobin in the bullfrog. J Gen Physiol 35: 23–40

Sasaki K, Sonoda Y (2000) Histometrical and three-dimensional analyses of liver hematopoiesis in the mouse embryo. Arch Histol Cytol 63: 137–146

Sawada K, Krantz SB, Kans JS, Dessypris EN, Sawyer S, Glick AD, Civin CI (1987) Purification of human erythroid colony-forming units and demonstration of specific binding of erythropoietin. J Clin Invest 80: 357–366

Shelly LL, Tynan W, Schmid W, Schutz G, Yeoh GC (1989) Hepatocyte differentiation in vitro: initiation of tyrosine aminotransferase expression in cultured fetal rat hepatocytes. J Cell Biol 109: 3403–3410

Suda T, Arai F, Hirao A (2005) Hematopoietic stem cells and their niche. Trends Immunol 26: 426–33

Tamura K, Takamatsu N, Ito M (2015) Erythropoietin protects red blood cells from TRAIL1-induced cell death during red blood cell transition in *Xenopus laevis*. Mol Cell Biochem 398(1–2): 73–81

Tanizaki Y, Ishida-Iwata T, Obuchi-Shimoji M, Kato T (2015) Cellular characterization of thrombocytes in *Xenopus laevis* with specific monoclonal antibodies. Exp Hematol 43: 125–136

Tavassoli M (1991) Embryonic and fetal hematopoiesis: an overview. Blood 17: 269–281

Thomas N, Maclean N (1975) The erythroid cell of anemic Xenopus laevis. I. Studies on cellular morphology and protein and nucleic acid synthesis during differentiation. J Cell Sci 19: 509–520

Turpen JB, Kelley CM, Mead PE, Zon LI (1997) Bipotential primitive-definitive hematopoietic progenitors in the vertebrate embryo. Immunity 7: 325–334

Wiechmann AF, Wirsig-Wiechmann C (2003) Color atlas of *Xenopus laevis* histology. Kluwer Academic Publishers, Berlin

(Received March 3, 2016 / Accepted July 6, 2016)